Journal of Engineering Science and Technology
Vol. 5, No. 2 (2010) 190 - 212

NUMERICAL SOLUTION OF STEADY STATE DISPERSION FLOW MODEL FOR LACTOSE-LACTASE HYDROLYSIS WITH DIFFERENT KINETICS IN FIXED BED

OLAOSEBIKAN ABIDOYE OLAFADEHAN[1,*], DAVID STAN ARIBIKE[1], ADEKUNLE MICHAEL ADEYEMO[2]

[1]Department of Chemical Engineering, University of Lagos, Nigeria
[2]Department of Chemical Engineering, Massachusetts Institute of Technology, USA
*Corresponding Author: oolafadehan@unilag.edu.ng

Abstract

A detailed computational procedure for evaluating lactose hydrolysis with immobilized enzyme in a packed bed tubular reactor under dispersion flow conditions is presented. The dispersion flow model for lactose hydrolysis using different kinetics, taking cognizance of external mass transfer resistances, was solved by the method of orthogonal collocation. The reliability of model simulations was tested using experimental data from a laboratory packed bed column, where the β-galactosidase of *Kluyveromyces fragilis* was immobilized on spherical chitosan beads. Comparison of the simulated results with experimental exit conversion shows that the dispersion flow model and using Michaelis-Menten kinetics with competitive product (galactose) inhibition are appropriate to interpret the experimental results and simulate the process of lactose hydrolysis in a fixed bed.

Keywords: Lactose hydrolysis, Immobilized enzyme, Dispersion flow, Orthogonal collocation, Michaelis-Menten, Competitive inhibition.

1. Introduction

Lactose is a disaccharide that makes up to 2-8% of the solid in milk. It consists of two subunits, galactose and glucose, linked together by a β-1,4-glycosidic bond. It occurs naturally only in milk hence it is commonly referred to as milk sugar. As a sugar, it is less sweet than its corresponding counterparts, maltose and sucrose, and as such it is widely used in baking and in commercial infant-milk formulas.

Nomenclatures

a	Surface area of particles per unit volume of packed bed, cm^2/cm^3
C_{Eo}	Initial enzyme concentration, g protein/g support weight
C_p	Concentration of product (galactose), mol/dm^3
C_S	Substrate (lactose) concentration, mol/dm^3
C_{Si}	Substrate (lactose) concentration on catalyst surface, mol/dm^3
C_{So}	Initial substrate concentration, mol/dm^3
$\overline{C}_S$	Dimensionless substrate concentration, C_S/C_{So}
D_L	Axial dispersion coefficient, cm^2/s
$D_{L,S}$	Substrate diffusion coefficient in water, cm^2/s
D_r	Radial diffusivity, cm^2/s
d_p	Diameter of particles, cm
d_r	Diameter of reactor, cm
F	Substrate input flow rate, ml/h
K_I	Product inhibition constant, mol/dm^3
K_M, K'_M	Michaelis-Menten constants, mol glucose/dm^3
k, k'	Rate constants for Michaelis-Menten without and with product inhibition, mol/(g protein.dm^3s)
k_o	Specific reaction rate constant for zero-order kinetics, mol/(dm^3s)
k_L	Mass transfer coefficient, cm/s
k_1	Specific reaction rate constant for first-order kinetics, s^{-1}
L	Length of reactor, cm
Pe	Peclet number, U_fL/D_L, dimensionless
Re	Reynolds number
r	Radial distance in the particle, cm
$(-r_S)$	Rate of reactant loss due to chemical reaction within the element of volume, mol/(dm^3s)
Sc	Schmidt number, $\mu_{L,S}/(\rho_{L,S}D_{L,S})$, dimensionless
S_D	Standard deviation
St	Modified Stanton number, k_LaL/U_f, dimensionless
t	Time, s
U_f	Superficial velocity of lactose solution, cm/s
u	Dimensionless axial distance, z/L
v_{max}, $v'_{\max}$	Maximum reaction velocity, mol/(dm^3s)
W_{sup}	Weight of support, g
XS	Fraction conversion of substrate, dimensionless
z	Axial distance in the reactor, cm

Greek Symbols

$\in_b$	Average void fraction of the packed bed, dimensionless
γ	Dimensionless substrate concentration with respect to surface concentration, C_{Si}/C_S
$\mu_{L,S}$	Viscosity of lactose solution, g/(cm s)
ρ_b	Bed density, g/cm^3
$\rho_{L,S}$	Density of lactose solution, g/cm^3
ρ_p	Particle density, g/cm^3

Lactose is produced industrially by concentrating whey, a by product of the manufacture of cheese. Traditionally, cheese whey has been considered a waste and the dairy industry tended to focus on its disposal. Current trends aim at the recovery of valuable components from whey or seek to utilize whey by other means. Cheese whey consists of the protein casein (solid) and the carbohydrate lactose (in solution). The protein fraction can be removed by concentrated ultra-filtration (UF) to produce whey protein concentrates and a lactose-rich UF permeate. Addition of β-galactosidase would hydrolyze the lactose in the whey to a mixture of monosaccharide - galactose and glucose, which are sweeter and more soluble. Use of lactose-hydrolyzed whey in ice cream would help to minimize the potential problems of sandy texture caused by the formation of lactose crystals while contributing to the sweetness. The low solubility of lactose limits the concentration of whey or permeate for transport. Lactose hydrolysis prior to the concentration process would allow for a higher degree of water removal thus lowering the cost of transportation. The resulting syrup could then be used to supplement or replace conventional sweeteners such as sucrose. Finally, the hydrolysis of lactose in many dairy products could make them available to consumers suffering from lactose intolerance. A potential market of some 50 million people was estimated to exist in the USA alone [1, 2]. So, lactose must be hydrolyzed into its monosaccharide components, allowing digestion which is the purpose of products today such as LACTAID.

The hydrolysis of lactose can be carried out using either acid hydrolysis or enzyme. Acid hydrolysis involves heating of lactose with simple acid reagents such as tetraoxosulphate (VI) acid, H_2SO_4, (free acid form) or acid form of a cationic exchange resin (a solid acid). This process, though simple, is however quite complex from a mechanistic perspective. This is partly due to the fact that the monosaccharide products can be further degraded into undesirable chemicals, wherein the number of possible side reactions depends upon, amongst other factors, the source of lactose and its composition e.g. whey permeate [3]. Lactose hydrolysis can be done either by using the enzyme in its free state or immobilized on a support. Immobilization is a method where an enzyme is imprisoned in another phase different from the substrate phase. The hydrolysis of lactose can be carried out using immobilized enzyme owing to its stability over broad ranges of pH and temperature, ability to stop reaction rapidly by removing the enzyme from the reaction solution, cheapness, ease of separation, high purity, and repeated usage capability. Free enzyme hydrolysis of lactose is not in use due to the fact that it is more expensive and can contaminate the final products with the introduction of foreign protein into them. Also, an immobilized enzyme can be used over a longer period than an enzyme solution thus lending itself for use in continuous processes.

The commercial enzymes used for lactose hydrolysis are β-galactosidases of diverse origins [4-6]. Jelen [7] proposed the use of sonicated dairy cultures to produce a relatively impure source of β-galactosidase for a potentially more economical process of lactose hydrolysis. Many studies have been made with β-galactosidases obtained from Escherichia coli, although their use is not viable for products intended for human consumption [8-12]. Yeast and fungal enzymes have the greatest commercial interests as they satisfy the specifications recommended for food enzymes. Yeast enzymes such as *Kluyveromyces fragilis* and *Kluyveromyces lactis* are habitually used for products with neutral pH values [13] such as milk and sweet whey. Fungal enzymes such as *Aspergillus niger* and

Aspergillus oryzae are usually used to hydrolyze lactose from products with acidic pH values, such as whey.

The type of reactor used almost exclusively in commercial applications for lactose hydrolysis is the packed bed reactor since it is easily automated, efficient, improves substrate conversion and needs little routine maintenance. Furthermore, it is more suitable than a continuous-flow stirred tank reactor especially when product inhibition is present in the enzyme reaction [14].

A great number of publications related to packed bed, immobilized enzyme reactors for lactose hydrolysis have described the development of different mathematical models that take into account mass transport equations according to the operating conditions, such as the hydrodynamic conditions, external and/or internal mass transfer resistance and the kinetic rate. These models apply only the simple Michaelis-Menten equation without product inhibition in the reaction kinetics [15], without comparative analyses with other kinetic reaction mechanisms. In some cases, model equations were theoretically solved following different approaches in order to simplify the problem. Consequently, some variables were neglected in order to obtain a simple equation that can be solved or adjusted so as to fit experimental data [16]. The kinetic constants and correlation of the mass transfer coefficient were modified. In other cases, the mass transfer resistance was not considered in the studies [17, 18]. Olafadehan et al. [19] reduced the mass transfer coefficient by a factor of 34.5 for the plug flow model for lactose hydrolysis in order to predict the experimental data.

The objective of this work is to develop a feasible and comprehensive mathematical model for lactose-lactase hydrolysis in a fixed bed reactor. Numerical solution of the resulting dispersion flow model, taking cognizance of external mass transfer resistances and using different kinetics for lactose hydrolysis by β-galactosidase of *Kluyveromyces fragilis* attached on spherical chitosan beads in a packed bed reactor was achieved by using orthogonal collocation method. The kinetics of the hydrolysis reaction and the flow inside the reactor were identified and thus the progress of hydrolysis rate and fractional conversion were determined.

2. Scope

The enzymatic hydrolysis of lactose is one of the most important biotechnological processes in the food industry. Design and analysis of such systems require identification of the flow system in a fixed bed. The objective of this study was to develop a feasible and comprehensive dispersion flow model for lactose-lactase hydrolysis in a fixed bed containing β-galactosidase immobilized on spherical chitosan beads, and the necessary numerical solution of orthogonal collocation method. Although many investigators have presented models for lactose-lactase hydrolysis in fixed beds, the model developed herein is the most comprehensive since it accounts for axial and radial dispersion effects, and chemical reaction. Comparative analyses of the dispersion and plug flow models for lactose-lactase hydrolysis with different kinetic reaction mechanisms, and taking into cognizance the effect of mass transfer resistances were exhaustively carried out in this study. The numerical solution developed permits detailed design and analysis of lactose-lactase hydrolysis in fixed bed under dispersion flow conditions.

3. Mathematical Model

Olafadehan [20] developed the continuity equation for an isothermal reaction occurring under diffusive conditions in a packed bed tubular reactor containing immobilised enzyme as

$$\frac{\partial C_S}{\partial t} = D_L \frac{\partial^2 C_S}{\partial z^2} - U_f \frac{\partial C_S}{\partial z} + D_r \left(\frac{\partial^2 C_S}{\partial r^2} + \frac{1}{r} \frac{\partial C_S}{\partial r} \right) - \left(- r_S \right) \tag{1}$$

Usually radial dispersion can be neglected in comparison with axial dispersion where the ratio of the column diameter to its length is very small (as is the case in this study) and flow is in the turbulent region [19]. When radial dispersion can be neglected in comparison with axial dispersion, Eq. (1) reduces to:

$$\frac{\partial C_S}{\partial t} = D_L \frac{\partial^2 C_S}{\partial z^2} - U_f \frac{\partial C_S}{\partial z} - \left(- r_S \right) \tag{2}$$

For steady state operation, we have:

$$D_L \frac{d^2 C_S}{dz^2} - U_f \frac{dC_S}{dz} - \left(- r_S \right) = 0 \tag{3}$$

subject to initial and boundary conditions:

$$C_S = C_{So}, \qquad L \geq z \geq 0 \tag{4}$$

$$C_S = C_{So} + \frac{D_L}{U_f} \frac{dC_S}{dz}, \qquad z = 0^+ \tag{5}$$

$$\frac{dC_S}{dz} = 0, \qquad z = L \tag{6}$$

Equation (5) is the famous Wehner and Wilhelm [21] boundary condition for the convective - diffusive problem. It is the appropriate boundary condition for the problem herein [22]. This states that for an imaginary line at the entrance of the reactor, the rate at which material crosses the line is in two parts: a convective part $\left(U_f C_S \right)$ and a diffusive part $\left(- D_L \frac{dC_S}{dz} \right)$, and that the two parts sum up to the material being fed into the reactor $\left(U_f C_{So} \right)$. Equation (6) represents the condition of no change in substrate concentration downstream of the reactor exit.

4. The Reaction Term, r_S

The general kinetics scheme that applies to hydrolysis of lactose with β-galactosidase immobilized on chitosan beads in a tubular fixed bed reactor is given thus [23]

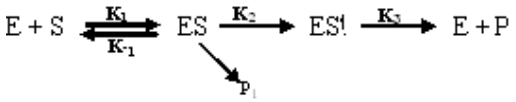

This involves rapid binding of the substrate, *S*, to yield the enzyme-substrate addition complex, *ES*; the formation of the glycosidyl-enzyme, ES', with the concomitant removal of glucose, *P1*, the moiety (ROH) of the substrate, and the hydrolysis of ES' to yield the second product (galactose, *P*) and free enzyme [23].

The kinetics considered for enzymatic hydrolysis of lactose by a β-galactosidase from *Kluyveromyces fragilis* are given thus:

(i) Zero-order kinetics: $\left(-r_S\right) = k_o$ (7)

(ii) First-order kinetics: $\left(-r_S\right) = k_1 C_{Si}$ (8)

(iii) Michaelis-Menten kinetics without inhibition: $\left(-r_S\right) = \dfrac{\nu_{\max} C_{Si}}{K_M + C_{Si}}$ (9)

(iv) Michaelis-Menten kinetics with competitive product (galactose) inhibition:

$$\left(-r_S\right) = \frac{\nu'_{\max} C_{Si}}{K'_M\left(1+\dfrac{C_P}{K_I}\right)+C_{Si}} \tag{10}$$

Equations (9) and (10) were obtained by applying quasi-steady-state approximation to the intermediates in the reaction scheme given above. However, Michaelis-Menten with competitive product inhibition is the most acceptable for working with product inhibition, which is the case of the proposed enzyme [24]. The product concentration, C_P, is stoichiometrically related to the substrate concentration, C_S, and change with the axial distance in the reactor, i.e. $C_P = C_{So} - C_S$. The consumption of the substrate at the interface has to be compensated for by transport from the bulk liquid. It is assumed that no partition effects exist [25] since the substrate has no net charge to modify the distribution between liquid and solid at interface. Hence, we have

$$\left(-r_S\right) = k_L a\left(C_S - C_{Si}\right) \tag{11}$$

where k_L is the mass transfer coefficient and *a* the surface area of particles per unit volume of packed bed, given by: $a = 6\left(1-\in_b\right)/d_p$.

Combining Eqs. (7) and (10) independently with Eq. (11), we have

For zero order kinetics, $\gamma = 1 - \dfrac{k_o}{k_L a C_S}$ (12)

For first order kinetics, $\gamma = \dfrac{k_L a}{k_1 + k_L a}$ (13)

For Michaelis-Menten kinetics without product inhibition,

$$\gamma = \frac{C_S - \phi - K_M + \sqrt{\left(\phi + K_M - C_S\right)^2 + 4K_M C_S}}{2C_S} \tag{14}$$

For Michaelis-Menten kinetics with competitive product inhibition,

$$\gamma = \frac{\alpha_1 C_S - \alpha_2 + \sqrt{(\alpha_2 - \alpha_1 C_S)^2 + 4C_S(\alpha_3 - \alpha_4 C_S)}}{2C_S} \tag{15}$$

where

$$\gamma = \frac{C_{Si}}{C_S},\ \phi = \frac{\nu_{\max}}{k_L a},\ \phi' = \frac{\nu'_{\max}}{k_L a}$$

$$\alpha_1 = \frac{K'_M}{K_I} + 1,\ \alpha_2 = \phi' + K'_M\left(\frac{C_{So}}{K_I} + 1\right),\ \alpha_3 = K'_M\left(\frac{C_{So}}{K_I} + 1\right),\ \alpha_4 = \frac{K'_M}{K_I}$$

Using Eq. (11) in Eq. (3), we have:

$$\frac{d^2C_S}{dz^2} - \frac{U_f}{D_L}\frac{dC_S}{dz} - \frac{k_L a C_S}{D_L}(1-\gamma) = 0 \tag{16}$$

which is the dispersion flow model for lactose-lactase hydrolysis in a fixed bed, taking into account external mass transfer resistance. For the case where external mass transfer resistance is neglected, the dispersion flow model for lactose-lactase hydrolysis using different kinetic equations is given by

For zero order kinetics: $$\frac{d^2C_S}{dz^2} - \frac{U_f}{D_L}\frac{dC_S}{dz} - \frac{k_o}{D_L} = 0 \tag{17}$$

For first order kinetics: $$\frac{d^2C_S}{dz^2} - \frac{U_f}{D_L}\frac{dC_S}{dz} - \frac{k_1}{D_L}C_S = 0 \tag{18}$$

For Michaelis-Menten kinetics without product inhibition:

$$\frac{d^2C_S}{dz^2} - \frac{U_f}{D_L}\frac{dC_S}{dz} - \frac{\nu_{\max}}{D_L}\frac{C_S}{K_M + C_S} = 0 \tag{19}$$

For Michaelis-Menten kinetics with competitive product inhibition

$$\frac{d^2C_S}{dz^2} - \frac{U_f}{D_L}\frac{dC_S}{dz} - \frac{\nu'_{\max}}{D_L}\frac{C_S}{K'_M\left(1 + \frac{C_{So} - C_S}{K_I}\right) + C_S} = 0 \tag{20}$$

Hence, the substrate concentration changes with axial distance in the reactor for dispersion flow model according to the rate of kinetic equations. Therefore, numerical solutions are sought for Eqs. (16)–(20) independently with the associated initial and boundary conditions.

5. Method of Numerical Solution

The mathematical model equations for the dispersion flow in the packed bed reactor involve a second-order ordinary differential equation. The numerical

technique adopted for its solution is the method of orthogonal or optimal collocation [19, 26]. The orthogonal collocation method is applied by first choosing a new set of dimensionless variables, which have values lying between 0 and 1. These variables are:

$$\overline{C}_S = \frac{C_S}{C_{So}} \text{ and } u = \left(\frac{z}{L}\right)^2$$

Therefore, Eq. (16) for case of external mass transfer resistance becomes:

$$\frac{4u}{\text{Pe}}\frac{d^2\overline{C}_S}{du^2} - 2\sqrt{u}\frac{d\overline{C}_S}{du} - \text{St}(1-\gamma)\overline{C}_S = 0 \tag{21}$$

where St is the modified Stanton number $\left(=k_L aL/U_f\right)$, a dimensionless mass transfer coefficient. Hence, the main Eq. (21) for dispersion flow model must be solved with Eqs. (12)–(15) independently for each kinetics in order to consider the γ variations as indicated. The resulting equations are presented thus:

For zero order kinetics: $$\frac{4u}{\text{Pe}}\frac{d^2\overline{C}_S}{du^2} - 2\sqrt{u}\frac{d\overline{C}_S}{du} - \Phi_1 = 0 \tag{22}$$

For first order kinetics: $$\frac{4u}{\text{Pe}}\frac{d^2\overline{C}_S}{du^2} - 2\sqrt{u}\frac{d\overline{C}_S}{du} - \Phi_2\overline{C}_S = 0 \tag{23}$$

For Michaelis-Menten kinetics without product inhibition:

$$\frac{4u}{\text{Pe}}\frac{d^2\overline{C}_S}{du^2} - 2\sqrt{u}\frac{d\overline{C}_S}{du} - \Phi_3\left[C_{So}\overline{C}_S + \phi + K_M - \sqrt{\left(\phi + K_M - C_{So}\overline{C}_S\right)^2 + 4K_M C_{So}\overline{C}_S}\right] = 0 \tag{24}$$

For Michaelis-Menten kinetics with competitive product inhibition:

$$\frac{4u}{\text{Pe}}\frac{d^2\overline{C}_S}{du^2} - 2\sqrt{u}\frac{d\overline{C}_S}{du} - \Phi_3\left[C_{So}\overline{C}_S(2-\alpha_1) + \alpha_2 - \sqrt{\left(\alpha_2 - \alpha_1 C_{So}\overline{C}_S\right)^2 + 4C_{So}\overline{C}_S\left(\alpha_3 - \alpha_4 C_{So}\overline{C}_S\right)}\right] = 0 \tag{25}$$

where $\Phi_1 = \dfrac{k_o L}{U_f C_{So}}$; $\Phi_2 = \dfrac{\text{St}k_1}{k_1 + k_L a}$; $\Phi_3 = \dfrac{\text{St}}{2C_{So}}$.

For the case where external mass transfer resistance is ignored, the dispersion flow model equation for each of the kinetics considered is presented thus:

For zero-order: $$\frac{4u}{\text{Pe}}\frac{d^2\overline{C}_S}{du^2} - 2\sqrt{u}\frac{d\overline{C}_S}{du} - \Phi_1 = 0 \tag{26}$$

For first-order: $$\frac{4u}{\text{Pe}}\frac{d^2\overline{C}_S}{du^2} - 2\sqrt{u}\frac{d\overline{C}_S}{du} - \Phi_4\overline{C}_S = 0 \tag{27}$$

For Michaelis-Menten kinetics without product inhibition:

$$\frac{4u}{\text{Pe}}\frac{d^2\overline{C}_S}{du^2} - 2\sqrt{u}\frac{d\overline{C}_S}{du} - \frac{\Phi_5\overline{C}_S}{\Phi_6 + \overline{C}_S} = 0 \tag{28}$$

For Michaelis-Menten kinetics with competitive product inhibition:

$$\frac{4u}{\mathrm{Pe}}\frac{d^2\overline{C}_S}{du^2} - 2\sqrt{u}\frac{d\overline{C}_S}{du} - \frac{\Phi_7\overline{C}_S}{\Phi_8+\Phi_9\overline{C}_S} = 0 \tag{29}$$

where

$$\Phi_4 = \frac{Lk_1}{U_f};\ \Phi_5 = \frac{L\nu_{\max}}{U_f C_{So}};\ \Phi_6 = \frac{K_M}{C_{So}};$$

$$\Phi_7 = \frac{L\nu'_{\max}}{U_f C_{So}};\ \Phi_8 = K'_M\left(\frac{1}{C_{So}}+\frac{1}{K_I}\right);\Phi_9 = 1 - \frac{K'_M}{K_I}$$

Each of the Eqs. (22)–(29) is subject to the transformed initial and boundary conditions

$$\overline{C}_S = 1, \qquad 1 \geq u \geq 0 \tag{30}$$

$$\overline{C}_S = 1 + \frac{2\sqrt{u}}{Pe}\frac{d\overline{C}_S}{du}, \qquad u = 0^+ \tag{31}$$

$$\frac{d\overline{C}_S}{du} = 0, \qquad u = 1 \tag{32}$$

It should be stated here that the dispersion flow model for lactose-lactase hydrolysis in a fixed bed is the same using zero order kinetics for both cases of excluding and including mass transfer resistance in the model (Eqs. (22) and (26)). When the method of orthogonal collocation is applied to the space variable u, Eqs. (22)–(25) for the case of mass transfer resistance become

$$\Phi_{10}\sum_{k=1}^{N+2} B_{j,k}\overline{C}_{Sk} - \Phi_{11}\sum_{k=1}^{N+2} A_{j,k}\overline{C}_{Sk} - \Phi_1 = 0 \quad j = 2,3\ldots..,N+1 \tag{33}$$

$$\Phi_{10}\sum_{k=1}^{N+2} B_{j,k}\overline{C}_{Sk} - \Phi_{11}\sum_{k=1}^{N+2} A_{j,k}\overline{C}_{Sk} - \Phi_2\overline{C}_{S\,j} = 0 \quad j = 2,3,..,N+1 \tag{34}$$

$$\Phi_{10}\sum_{k=1}^{N+2} B_{j,k}\overline{C}_{Sk} - \Phi_{11}\sum_{k=1}^{N+2} A_{j,k}\overline{C}_{Sk} - \Phi_3 f\left(\overline{C}_{S\,j}\right) = 0 \quad j = 2,3,.,N+1 \tag{35}$$

$$\Phi_{10}\sum_{k=1}^{N+2} B_{j,k}\overline{C}_{Sk} - \Phi_{11}\sum_{k=1}^{N+2} A_{j,k}\overline{C}_{Sk} - \Phi_3 g\left(\overline{C}_{S\,j}\right) = 0 \quad j = 2,3.,N+1 \tag{36}$$

while for the case of ignoring mass transfer resistance, Eqs. (27)–(29) become

$$\Phi_{10}\sum_{k=1}^{N+2} B_{j,k}\overline{C}_{Sk} - \Phi_{11}\sum_{k=1}^{N+2} A_{j,k}\overline{C}_{Sk} - \Phi_4\overline{C}_{S\,j} = 0 \quad j = 2,3,.,N+1 \tag{37}$$

$$\Phi_{10}\sum_{k=1}^{N+2} B_{j,k}\overline{C}_{Sk} - \Phi_{11}\sum_{k=1}^{N+2} A_{j,k}\overline{C}_{Sk} - \frac{\Phi_5\overline{C}_{S\,j}}{\Phi_6+\overline{C}_{Sj}} = 0 \quad j = 2,3,,N+1 \tag{38}$$

$$\Phi_{10}\sum_{k=1}^{N+2} B_{j,k}\overline{C}_{Sk} - \Phi_{11}\sum_{k=1}^{N+2} A_{j,k}\overline{C}_{Sk} - \frac{\Phi_7\overline{C}_{S\,j}}{\Phi_8+\Phi_9\overline{C}_{Sj}} = 0 \quad j = 2,3,,N+1 \tag{39}$$

where $\Phi_{10} = 4u_j / \mathrm{Pe}$, $\Phi_{11} = 2\sqrt{u_j}$,

$$f\left(\overline{C}_{Sj}\right) = C_{So}\overline{C}_{Sj} + \phi + K_M - \sqrt{\left(\phi + K_M - C_{So}\overline{C}_{Sj}\right)^2 + 4K_M C_{So}\overline{C}_{Sj}}$$

and $$g\left(\overline{C}_{Sj}\right) = C_{So}\overline{C}_{Sj}\left(2-\alpha_1\right) + \alpha_2 - \sqrt{\left(\alpha_2 - \alpha_1 C_{So}\overline{C}_{Sj}\right)^2 + 4C_{So}\overline{C}_{Sj}\left(\alpha_3 - \alpha_4 C_{So}\overline{C}_{Sj}\right)}$$

The initial and boundary conditions are transformed as follows:

$$\overline{C}_{Sj} = 1 \qquad j = 1, 2, \ldots\ldots\ldots, N+2, \ \tau \le 0 \tag{40}$$

$$\overline{C}_{S1} = 1 + \frac{\Phi_{11}}{Pe}\sum_{k=1}^{N+2} A_{1,k}\overline{C}_{Sk} \qquad u = 0^+ \tag{41}$$

$$\sum_{k=1}^{N+2} A_{N+2,k}\,\overline{C}_{Sk} = 0 \qquad u = 1 \tag{42}$$

N is the number of interior collocation points in the axial direction. The two extra points have been included to incorporate the boundary conditions at the inlet and outlet of the fixed bed reactor. It should be noted that the boundary points $u = 0$ and $u = 1$ are taken as external collocation points in Eqs. (33) – (39).

Equations (41) and (42) are used to reduce the number of terms in the summations in Eqs. (33) – (39) such that it is taken from $k = 2$ to $k = N+1$ by the following procedure. First, Eqs. (41) and (42) are solved for $\overline{C}_{S1}$ and $\overline{C}_{SN+2}$ to obtain the following expressions:

$$\overline{C}_{S1} = \mathrm{Pe}' + \Phi_{11}\sum_{k=2}^{N+1} A'_{1,k}\overline{C}_{Sk} \tag{43}$$

$$\overline{C}_{SN+2} = \mathrm{Pe}'' + \sum_{k=2}^{N+1} A''_{1,k}\overline{C}_{Sk} \tag{44}$$

where

$$\mathrm{Pe}' = \frac{\dfrac{\mathrm{Pe}}{A_{1,N+2}}}{\dfrac{\mathrm{Pe}}{A_{1,N+2}} - \dfrac{\Phi_{11}A_{1,1}}{A_{1,N+2}} + \dfrac{\Phi_{11}A_{N+2,1}}{A_{N+2,N+2}}} \tag{45}$$

$$A'_{1,k} = \frac{\dfrac{A_{1,k}}{A_{1,N+2}} - \dfrac{A_{N+2,k}}{A_{N+2,N+2}}}{\dfrac{Pe}{A_{1,N+2}} - \dfrac{\Phi_{11}A_{1,1}}{A_{1,N+2}} + \dfrac{\Phi_{11}A_{N+2,1}}{A_{N+2,N+2}}} \tag{46}$$

$$\mathrm{Pe}'' = \frac{\dfrac{\mathrm{Pe}}{\Phi_{11}A_{1,1} - \mathrm{Pe}}}{\dfrac{A_{N+2,N+2}}{A_{N+2,1}} - \dfrac{\Phi_{11}A_{1,N+2}}{\Phi_{11}A_{1,1} - \mathrm{Pe}}} \tag{47}$$

$$A''_{1,k} = \frac{\dfrac{\Phi_{11}A_{1,k}}{\Phi_{11}A_{1,1} - \mathrm{Pe}} - \dfrac{A_{N+2,k}}{A_{N+2,1}}}{\dfrac{A_{N+2,N+2}}{A_{N+2,1}} - \dfrac{\Phi_{11}A_{1,N+2}}{\Phi_{11}A_{1,1} - Pe}} \tag{48}$$

Use of these expressions; Eqs. (43) and (44) to eliminate the concentrations at $u = 0$ and $u = 1$ from Eqs. (33)–(39) results in a reduction of the number of terms in the summations. After the above substitutions have been made, the summations in Eqs. (33)–(39) for different kinetics run from $k = 2$ to $k = N + 1$.

The resulting forms of these equations for lactose hydrolysis in a fixed bed containing β-galactosidase immobilised on chitosan beads using different kinetic reaction mechanisms are presented thus:

$$F_j = \sum_{k=2}^{N+1} T_{j,k}\overline{C}_{Sk} + d_j + Q\left(\overline{C}_{Sj}\right) = 0 \tag{49}$$

where

$$T_{j,k} = \Phi_{10}\left(B_{j,N+2}A''_{1,k} + \Phi_{11}B_{j,1}A'_{1,k} + B_{j,k}\right) - \Phi_{11}\left(A_{j,N+2}A''_{1,k} + \Phi_{11}A_{j,1}A'_{1,k} + A_{j,k}\right) \tag{50}$$

$$d_j = \Phi_{10}\left(B_{j,N+2}Pe'' + B_{j,1}Pe'\right) - \Phi_{11}\left(A_{j,N+2}Pe'' + A_{j,1}Pe'\right) \tag{51}$$

and when mass transfer resistance is considered,

$$Q\left(\overline{C}_{Sj}\right) = -\Phi_1 \text{ for zero-order kinetics} \tag{52}$$

$$Q\left(\overline{C}_{Sj}\right) = -\Phi_2\overline{C}_{Sj} \text{ for first-order kinetics} \tag{53}$$

for Michaelis-Menten kinetics without product inhibition

$$Q\left(\overline{C}_{Sj}\right) = -\Phi_3 f\left(\overline{C}_{Sj}\right) \tag{54}$$

for Michaelis-Menten kinetics with competitive product inhibition

$$Q\left(\overline{C}_{Sj}\right) = -\Phi_3 g\left(\overline{C}_{Sj}\right) \tag{55}$$

When mass transfer resistance is ignored, we have

$$Q\left(\overline{C}_{Sj}\right) = -\Phi_4\overline{C}_{Sj} \text{ for first-order kinetics} \tag{56}$$

for Michaelis-Menten kinetics without product inhibition

$$Q\left(\overline{C}_{Sj}\right) = -\frac{\Phi_5\overline{C}_{Sj}}{\Phi_6 + \overline{C}_{Sj}} \tag{57}$$

for Michaelis-Menten kinetics with competitive product inhibition

$$Q\left(\overline{C}_{Sj}\right) = -\frac{\Phi_7 \overline{C}_{Sj}}{\phi_8 + \Phi_9 \overline{C}_{Sj}} \tag{58}$$

So, the product concentration, $C_{Pj} = C_{So}\left(1 - \overline{C}_{Sj}\right)$, and the fractional conversion, $X_{Sj} = 1 - \overline{C}_{Sj}$.

Estimation of film mass transfer coefficients

The external mass transfer coefficient, k_L, was estimated by the Chilton and Colburn correlation given by [27]:

$$k_L = \frac{1.09}{\in_b} \frac{\left(D_{L,S}\right)^{\frac{2}{3}}}{d_p^g} \left(\frac{\rho_{L,S}}{\mu_{L,S}}\right)^{\frac{2}{3}-g} \left(U_f\right)^{1-g} \tag{59}$$

where $\in_b$ is the average void fraction of packed bed reactor, $D_{L,S}$ the liquid phase diffusivity of lactose, d_p the particle diameter, $\rho_{L,S}$ and $\mu_{L,S}$ the density and viscosity of the lactose solution respectively. The average g value is $2/3$ recommended for $0.0016 \leq Re \leq 55$ and $165 \leq Sc \leq 706000$ [17]. Using the experimental conditions, the calculated Reynolds and Schmidt numbers in this study fall within these respective ranges (Table 1) hence the justification for the use of $g = 2/3$. Hence, the mass transfer coefficient is independent of the density and viscosity of the lactose solution.

Table 1. Physical Parameters of the System as a Function of U_f at Different Initial Substrate Concentrations.

U_f (cm/s)	Pe	k_L (cm/s)	C_{So}=0.073 M, $\rho_{L,S}$ = 1.025 g/cm^3		C_{So}=0.146 M, $\rho_{L,S}$ = 1.05 g/cm^3		C_{So}=0.219 M, $\rho_{L,S}$ = 1.075 g/cm^3		C_{So}=0.292 M, $\rho_{L,S}$ = 1.10 g/cm^3	
			Re	Sc	Re	Sc	Re	Sc	Re	Sc
0.034	12.66	0.0396	0.7667	4.8485	0.7853	4.7332	0.8040	4.6233	0.8227	4.5184
0.039	14.56	0.0419	0.8794	4.7712	0.9008	4.6577	0.9223	4.5495	0.9437	4.4463
0.049	18.36	0.0450	1.1049	4.8050	1.1318	4.6907	1.1587	4.5818	1.1857	4.4778
0.059	22.16	0.0478	1.3304	4.8161	1.3628	4.7016	1.3952	4.5924	1.4276	4.4882
0.067	24.06	0.0500	1.5108	4.7973	1.5476	4.6832	1.5844	4.5744	1.6212	4.4706
0.078	27.86	0.0525	1.7588	4.8108	1.8017	4.6965	1.8445	4.5874	1.8874	4.4832
0.097	35.46	0.0566	2.1873	4.7926	2.2406	4.6787	2.2938	4.5700	2.3471	4.4663
0.119	45.12	0.0604	2.6834	4.8154	2.7487	4.7009	2.8141	4.5917	2.8794	4.4875

6. Simulation Results and Discussion

The dispersion flow model obtained in this study was solved using the orthogonal collocation method with N interior points. This method is based on expanding the variable C_S in terms of u_j^* using a series of known functions C_{S_j} to obtain an approximate solution to the differential equation in the domain $u_j^*(0,1)$.

In the orthogonal collocation method, the collocation points, which are the zeros of the Jacobi polynomial, are automatically picked by requiring that the polynomial must be orthogonal to each other so that for a set of N interior points, the series C_{Sj} are the exact solution with a weighted residual equal zero. The coefficients $\{A_{j,k}\}$ and $\{B_{j,k}\}$ of matrices **A** and **B** were evaluated on the basis of power series in the concentration. The orthogonal polynomial was taken to be the Jacobi polynomial $P_N^{(\alpha,\beta)}(u) = P_N^{(0,0)}(u)$ of order N=8, and weighting function, $W(u) = (1-u)^{\alpha} u^{\beta} = (1-u)^0 u^0 = 1$ as this value gives faster convergence [26]. The roots of the Jacobi polynomial were taken as the interior collocation points. The approximation order N of the orthogonal polynomial was tested with N=4, 6, 8, 10. N=8 proved to be sufficient to obtain differences in only the fourth digit in the predictions of concentration as compared to the higher and lower approximation. However, to solve the system of algebraic equations that were obtained, the Gaussian elimination method was used. Gauss-Siedel iteration scheme is not recommended because several iterations will generally be required for satisfactory convergence.

In the experimental work of Carrara and Rubiolo [28], a 14.0 cm × 1.2 cm column was used as the isothermal packed bed reactor at 43^{O}C, with a water recirculation jacket and a heating water bath, wherein β-galactosidase was immobilised on spherical chitosan beads using glutaraldehyde [29]. The beads had an average diameter, d_p of 0.22 cm and a density, ρ_p, of 1.102 g/cm^3. The kinetic constants were obtained in a batch system from an experimental data series with different initial substrate concentrations, determined under negligible internal mass transfer limitations [30]. Also, experimental exit conversion values were obtained for different inlet feed flows at four initial substrate concentrations for the reactor at steady state. Hence, their experimental data are appropriate to be used in this study and to which the predicted exit conversion was compared. No comparison could be done for the hydrolysis rate and fractional conversion along the length of the reactor as there are no published experimental data on these till date. Also, Carrara and Rubiolo [29] failed to report the hydrolysis rate and fractional conversion values along the length of the reactor, which are presented in the present study. The validity of the proposed model was ascertained through the excellent agreement between the predicted results obtained herein and experimental data of Carrara and Rubiolo [28].

The parameter values and kinetic constants used in this simulation are as follows [29,30]:

L=14.0 cm, ϵ_b = 0.389, d_r = 1.2 cm, $\rho_b = \rho_p (1-\epsilon_b)$ = 0.6733 g/cm^3, C_{Eo} = 0.021 g protein/g support weight, $D_{L,S}$ = 2.0296 × 10^{-3} cm^2/s, $k_o = v_{max} = kC_{Eo}W_{sup}$, $k_1 = v_{max}/K_M$, k = 1.01×10^{-2} mol/(g protein.dm^{3}s), $k' = 1.01\times10^{-2}$ mol/(g protein. dm^{3}s), K_M = 0.141 mol glucose/dm^3, K'_M = 0.137 mol glucose/dm^3 and K_1= 0.234 mol/dm^3.

So, it should be noted that according to the Michaelis-Menten mechanism, when $C_S > K_M$, $(-r_S) \approx v_{max} = k_o$, zero order kinetics is obtained. When $C_S < K_M$, $(-r_S) \approx (v_{max}/K_M) C_{Si}$ (or $k_1 C_S$), first order kinetics is obtained for cases of external and no external mass transfer resistances respectively. Lactose solution concentrations of 0.073, 0.146, 0.219 and 0.292 mol/dm^3 were used at a constant

flow rate between 113.0 and 483.0 ml/h. The weight of the chitosan beads, W_{sup}=10.66 g, and the maximum velocities for a support weight were $v_{max} = kC_{Eo}W_{sup}$ and $v'_{max} = k'C_{Eo}W_{sup}$ for Michaelis-Menten (herein referred to as M-M in all figures presented) without inhibition and with inhibition respectively.

Figures 1–4 show the comparison between the experimental and simulated exit conversion obtained for different inlet feed flows at four initial substrate concentrations of 0.073, 0.146, 0.219 and 0.292 mol/dm^3 using different kinetics for lactose hydrolysis when external mass transfer resistance was considered and neglected. The simulated results for lactose hydrolysis using zero-order kinetics for both cases of including and excluding mass transfer resistance in the dispersion flow model were not presented in these figures since no reasonable results were obtained, that is negative dimensionless substrate concentration values were obtained, which thus resulted in values of the exit conversion being greater than 1 for both cases of ignoring and taking into account external mass transfer resistances in the dispersion flow model. Therefore, the approximation of the Michaelis-Menten kinetics (i.e., the reaction term) to zero order resulted in very poor agreements to experimental data. Hence the zero order model is not applicable to such system. From Eq. (8), the reaction rate is proportional to the concentration changes, the first-order kinetics shows the most detectable variation of substrate concentration amongst the kinetics considered at higher concentrations. It needs to be mentioned that same values of $\overline{C}_S$ and fractional conversion were obtained using first-order kinetics at different initial substrate concentrations when external mass transfer resistance was considered in the dispersion flow model. Also, same values of these dependent variables were obtained when external mass transfer resistance was ignored in the dispersion flow model. This is indicative of the fact that the dispersion flow model is independent of the initial substrate concentration when first-order kinetics is used.

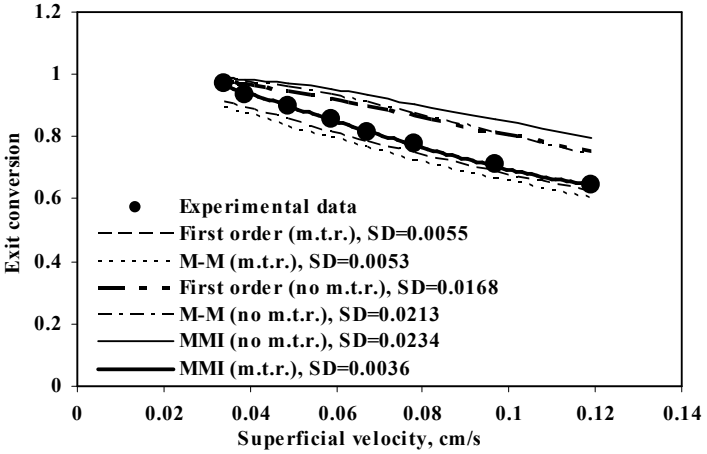

Fig. 1. Comparision of Experimental and Simulated Exit Conversion at Varying Superficial Velocity for Lactose using Different Kinetics when C_{so}= 0.073.

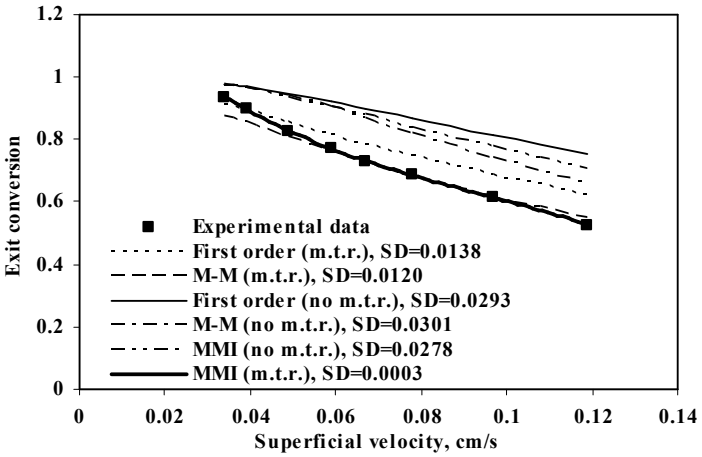

Fig. 2. Comparision of Experimental and Simulated Exit Conversion at Varying Superficial Velocity for Lactose using Different Kinetics when C_{so}= 0.146.

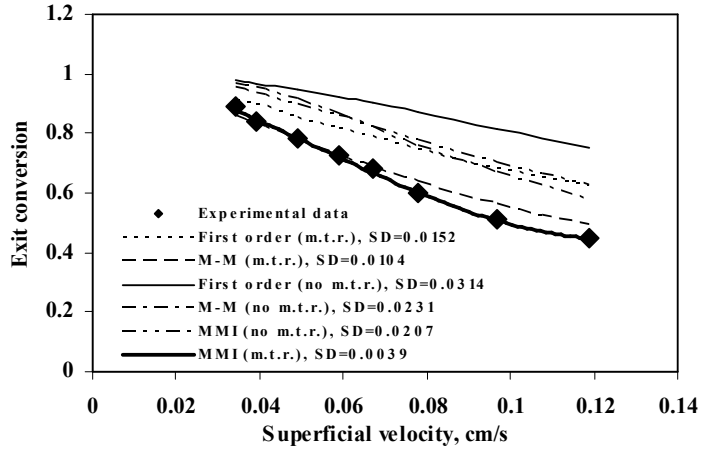

Fig. 3. Comparision of Experimental and Simulated Exit Conversion at Varying Superficial Velocity for Lactose using Different Kinetics when C_{so}= 0.219.

Figures 1–4 also reveal that the predicted results obtained by using first-order kinetics for lactose hydrolysis for both cases of ignoring and including external mass transfer resistance in the dispersion flow model do not agree with the experimental data. So, the simplification of the Michaelis-Menten equation to first-order kinetics when $K_M > C_S$ at the initial substrate concentration could not

be used for lactose hydrolysis, which is in agreement with the results of Hassan and Beg [31].

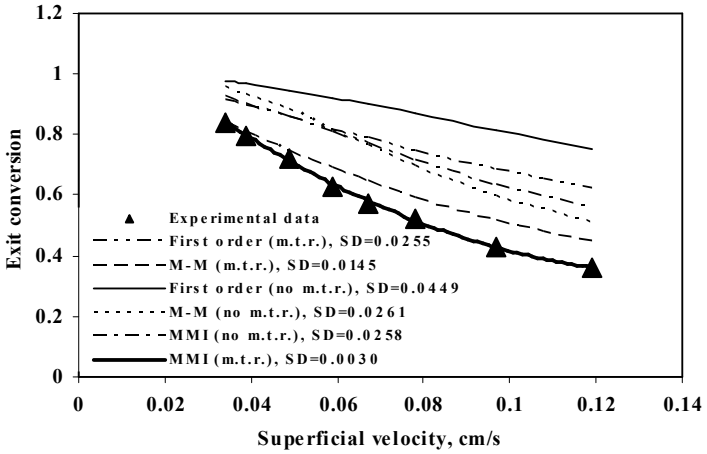

Fig. 4. Comparision of Experimental and Simulated Exit Conversion at Varying Superficial Velocity for Lactose using Different Kinetics when C_{so}= 0.292.

Even though, higher conversion values were obtained on using first-order kinetics than on using Michaelis-Menten without inhibition and Michaelis-Menten kinetics with competitive product inhibition, the predicted conversion values for Michaelis-Menten kinetics without inhibition are higher than experimental values since the product inhibition that reduces the substrate access to active sites of enzyme was not considered in the model. As it can be seen from Figs. 1–4, none of the predicted results for Michaelis-Menten kinetics without inhibition for both cases of excluding and including mass transfer resistance in the dispersion flow model agree with the experimental data. However, an excellent agreement between the experimental and predicted exit conversion was achieved for the case of Michaelis-Menten with competitive product inhibition when external mass transfer resistance was included in the dispersion flow model for lactose hydrolysis in a fixed bed containing β-galactosidase immobilised on chitosan beads. Moreover, the standard deviation (S_D) values computed for the different kinetic mechanisms with and without external mass transfer resistance were shown in Figs. 1–4. These figures reveal that the simulated results for lactose hydrolysis using Michaelis-Menten kinetics with competitive product inhibition when external mass transfer resistance was accounted for in the dispersion flow model had the smallest S_D values at all the initial substrate concentrations used in this study.

Tables 2–5 give the residual values (which are the differences between experimental and predicted exit fractional conversion) for all concentrations based on a dimensional conversion values (between 0 and 1). The lower the residual values, the better the fit. It is observed that generally the simulated results obtained using Michaelis-Menten kinetics with competitive product inhibition when external mass transfer resistance was included in the dispersion flow model gave the smallest residual values, followed by the Michaelis-Menten kinetics without inhibition while the first-order kinetics gave the largest residual values.

Table 2. Residual Values for each Kinetics when C_{So} = 0.073 mol/dm^3.

U_f	Residuals, C_{So} =0.073 mol/dm^3					
(cm/s)	With Mass Transfer Resistance			Without Mass Transfer Resistance		
	FIRST	M-M	MMI	FIRST	M-M	MMI
0.034	0.0591	0.0802	0.0004	-0.0086	-0.0161	-0.0192
0.039	0.0423	0.0634	-0.0008	-0.0323	-0.0407	-0.0462
0.049	0.0417	0.0628	-0.0003	-0.0507	-0.0608	-0.0713
0.059	0.0382	0.0592	-0.0005	-0.0680	-0.0782	-0.0950
0.067	0.0303	0.0526	-0.0008	-0.0842	-0.0931	-0.1158
0.078	0.0310	0.0534	-0.0002	-0.0916	-0.0973	-0.1284
0.097	0.0262	0.0481	0.0104	-0.1026	-0.1007	-0.1454
0.119	0.0232	0.0446	0.0003	-0.1066	-0.0951	-0.1525

Table 3. Residual Values for each Kinetics when C_{So} =0.146 mol/dm^3.

U_f	Residuals, C_{So} =0.146 mol/dm^3					
(cm/s)	With Mass Transfer Resistance			Without Mass Transfer Resistance		
	FIRST	M-M	MMI	FIRST	M-M	MMI
0.034	0.0259	0.0615	0.0007	-0.0398	-0.0405	-0.0357
0.039	0.0034	0.0423	-0.0004	-0.0712	-0.0699	-0.0652
0.049	-0.0272	0.0184	1E-05	-0.1196	-0.1110	-0.1090
0.059	-0.0461	0.0058	-0.0002	-0.1523	-0.1324	-0.1361
0.067	-0.0542	0.0038	0.0000	-0.1687	-0.1376	-0.1476
0.078	-0.0613	0.0022	-0.0001	-0.1839	-0.1367	-0.1562
0.097	-0.0711	-0.0010	-0.0003	-0.1999	-0.1270	-0.1622
0.119	-0.0957	-0.0212	0.0001	-0.2255	-0.1298	-0.1787

From the analyses above, it can be deduced that the kinetics of lactose hydrolysis by β-galactosidase of *Kluyveromyces fragilis* immobilised on spherical chitosan beads can be well represented by Michaelis-Menten kinetics with competitive product (galactose) inhibition, taking cognizance of external mass transfer resistance. The effect of the mass transfer was to reduce the effect of the flow rate so higher conversion values were obtained for all the kinetics considered when mass transfer resistance was ignored in the dispersion flow model than for the case of accounting for mass transfer resistance. However, the application of the Michaelis-Menten kinetics, Michaelis-Menten kinetics with competitive product inhibition, the approximation of the Michaelis-Menten kinetics to zero or first order to the dispersion flow model results in poor agreement with the experimental exit conversion data when mass transfer resistances were not included in the model (Figs. 1–4), as shown in their respective residual values presented in Tables 2- 5

In the experimental assays, the Peclet number, Pe, values changed from 12.66 to 45.11 according to superficial velocity. Hence, for the range of Pe numbers used, the axial dispersion model for lactose hydrolysis using Michaelis-Menten kinetics with competitive product inhibition without adjustment of mass transfer coefficient predicted the experimental data with higher accuracy than with the plug flow model for both cases of no adjustment and adjustment of mass transfer coefficient, which was considered by Olafadehan [19]. Figure 5 is typical of the plots obtained at the four substrate concentrations used in this study when comparison was made

between the experimental and simulated exit conversion for lactose hydrolysis using Michaelis-Menten kinetics with competitive product inhibition.

Table 4. Residual Values for each Kinetics when C_{So} =0.219 mol/dm^3.

U_f	Residuals, C_{So} =0.219 mol/dm^3					
(cm/s)	With Mass Transfer Resistance			Without Mass Transfer Resistance		
	FIRST	M-M	MMI	FIRST	M-M	MMI
0.034	-0.0209	0.0320	-0.0001	-0.0867	-0.0785	-0.0617
0.039	-0.0537	0.0065	0.0006	-0.1283	-0.1136	-0.0958
0.049	-0.1137	-0.0009	0.0040	-0.1677	-0.1336	-0.1186
0.059	-0.1303	-0.0044	0.0028	-0.1980	-0.1387	-0.1321
0.067	-0.1368	-0.0107	0.0010	-0.2201	-0.1400	-0.1425
0.078	-0.1460	-0.0376	0.0000	-0.2686	-0.1600	-0.1748
0.097	-0.1748	-0.0546	0.0094	-0.3036	-0.1568	-0.1900
0.119	-0.1728	-0.0457	-0.0004	-0.3026	-0.1277	-0.1747

Table 5. Residual Values for each Kinetics when C_{So} =0.292 mol/dm^3.

U_f	Residuals, C_{So} =0.292 mol/dm^3					
(cm/s)	With Mass Transfer Resistance			Without Mass Transfer Resistance		
	FIRST	M-M	MMI	FIRST	M-M	MMI
0.034	-0.0729	0.0004	0.0005	-0.1386	-0.1187	-0.0884
0.039	-0.0977	-0.0128	-0.0021	-0.1723	-0.1395	-0.1086
0.049	-0.1333	-0.0262	-0.0080	-0.2257	-0.1586	-0.1343
0.059	-0.1868	-0.0603	0.0000	-0.2930	-0.1864	-0.1756
0.067	-0.2170	-0.0786	0.0010	-0.3301	-0.1956	-0.1996
0.078	-0.2250	-0.0702	-0.0001	-0.3476	-0.1747	-0.1912
0.097	-0.2538	-0.0845	0.0001	-0.3826	-0.1661	-0.2017
0.119	-0.2608	-0.0848	0.0020	-0.3906	-0.1468	-0.1945

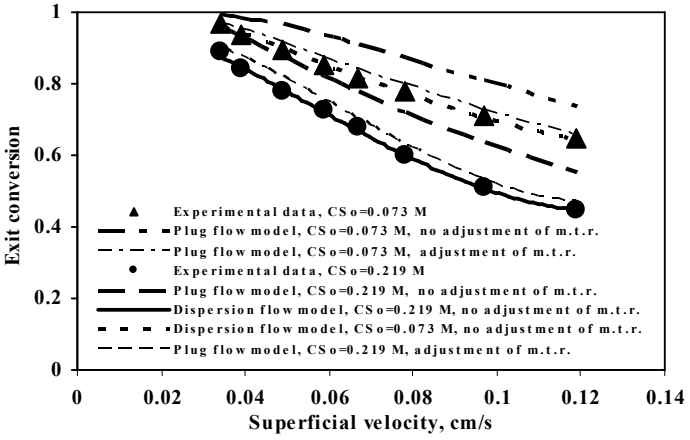

Fig. 5. Comparision of Experimental and Simulated Exit Conversion for Plug and Dispersion Flow Model for Lactose Hydrolysis using Michaelis-Menten Kinetics with Competitive Product Inhibition for C_{so}= 0.073 and 0.219 M.

Figures 6-8 depict the typical plots obtained for the progress of hydrolysis of lactose by β-galactosidase of *Kluyveromyces fragilis* at varying initial substrate concentrations and superficial velocities using Michaelis-Menten kinetics with competitive product inhibition when external mass transfer resistance was included in the dispersion flow model. The concentration of lactose was found to decrease with increasing axial distance in the reactor for all the kinetic equations,

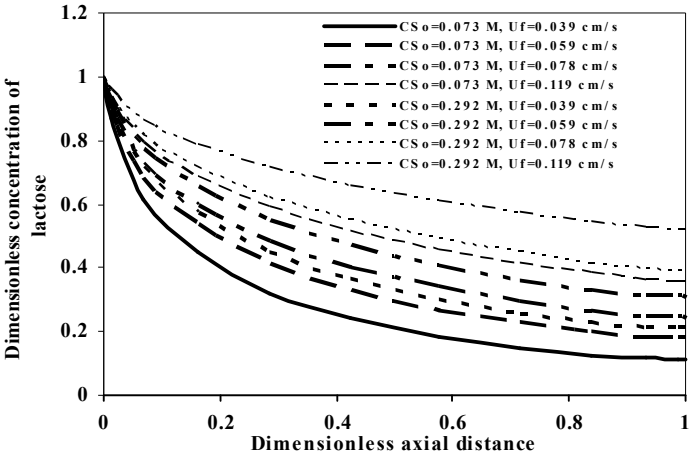

Fig. 6. Dimensionless Concentration of Lactose Against Dimensionless Axial Distance at Varying Superficial Velocity for C_{so}= 0.073 M and 0.292 M using Michaelis-Menten Kinetics with Inhibition when Mass Transfer Resistance is not Neglected.

except for zero-order kinetics, which gave negative results, so its simulated results need not be presented. However, simulated results of the dispersion flow model for lactose-lactase hydrolysis in a fixed bed were presented using Michaelis-Menten kinetics with competitive product inhibition at initial substrate concentrations of 0.073 and 0.292 M and varying superficial velocities (Fig. 6) since this is the only kinetics that correlated the experimental data excellently, amongst the different kinetics considered in this study. From Fig. 6, it was seen that the higher the flow rates, the steeper the plots, so higher substrate concentration values were obtained at higher flow rates at a particular initial substrate concentration, which thus led to lower product concentration values at higher flow rates (Fig. 7). Also, at lower flow rates and at a particular initial substrate concentration, it was observed that the substrate concentration profiles approach exponential trend more than at higher flow rates, and the system approaches steady states at the latter conditions more readily than at the former conditions. The decreasing trend of substrate concentration with increasing axial distance is expected as mass is carried from the entrance of the reactor, u = 0, towards the reactor exit, u=1, by convective transport and diffusion. Consequently, $\overline{C}_S$ decreases in this direction as u increases.

Figure 6 is also indicative of the fact that higher conversion values were obtained at lower flow rates at a particular substrate concentration, as revealed in

Fig. 8. This ought to be expected, as the enzyme activity loss is less at lower flow rates than at higher flow rates. This is due to the fact that increase in the substrate flow rates increases the superficial velocities of the fluid. Hence, agitation in the reactor increases, which now results in more attrition of the binder on the support, and thus the release of more enzymes to be carried out of the reactor.

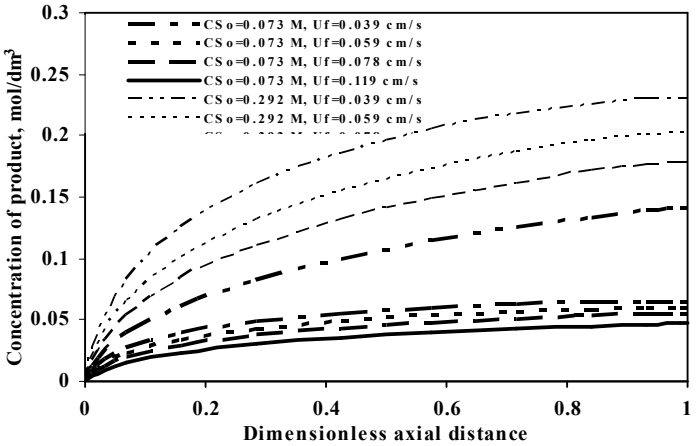

Fig. 7. Concentration of Product (Galactose) against Dimensionless Axial Distance at Varying Superficial Velocity for C_{so}= 0.073 and 0.292 M using Michaelis-Menten Kinetics with Inhibition when External Mass Transfer Resistance is not Neglected.

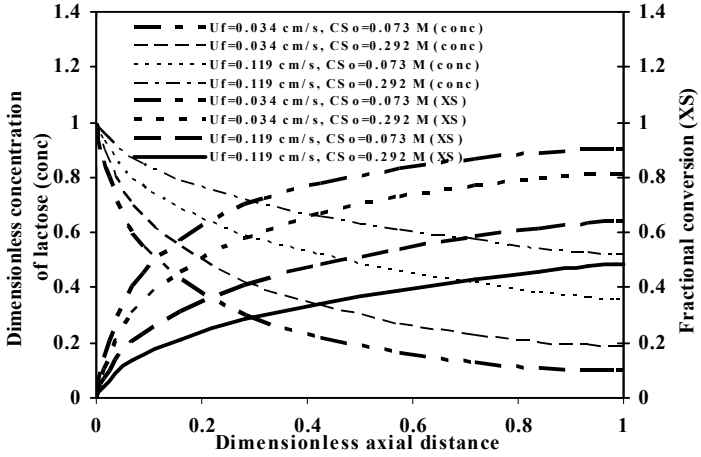

Fig. 8. Dimensionless Lactose Concentration and Fractional Conversion against Dimensionless Axial Distance for Varying C_{so} at U_f = 0.034, 0.119 cm/s using Michaelis-Menten Kinetics with Inhibition when External Mass Transfer Resistance is not Neglected.

7. Conclusions

A mathematical model void of significant radial dispersion effects and internal diffusion resistances and based on different kinetics for lactose hydrolysis in a fixed bed was solved using the method of orthogonal collocation. Excellent agreement was achieved between the experimental and predicted exit conversion for the case of Michaelis-Menten kinetics with competitive product (galactose) inhibition when external mass transfer resistance was included in the dispersion flow model. Hence, the kinetics of lactose conversion by β-galactosidase of *Kluyveromyces fragilis* immobilised on spherical chitosan beads includes a product inhibition term. The dispersion flow model and Michaelis-Menten kinetics with competitive product inhibition can therefore be used as a design tool to predict the effects of varying operating conditions (initial substrate concentration, superficial velocity/substrate input flow rate) on reactor performance. The results of this study not only provide numerical solutions but also an exhaustive understanding of the reaction systems.

References

1. Sloan, A.E. (1999). The new market: foods for the not-so-healthy. *Food Technology*, 53(2), 54-60.
2. Bury, D.; and Jelen, P. (2000). Lactose hydrolysis using a disrupted dairy culture: evaluation of technical and economical feasibility. *Canadian Agricultural Engineering,* 42(2), 75-80.
3. Cote, A.; Brown, W.A.; Cameron, D.; and Van Walsum, G.P. (2004). Hydrolysis of lactose in whey permeate for subsequent fermentation to ethanol. *Journal of Dairy Science,* 87(6), 1608-1620.
4. Finocchiaro, F.; Olson, N.F.; and Richardson, T. (1980). Use of immobilised lactase in milk systems. *Advanced Biochemical Engineering,* 15, 71-88.
5. Ryder, D.N. (1989). Hydrolysis of lactose in whey products. *Bulletin of the International Dairy Federation,* 233, 45-52.
6. Zadow, J.G. (1992). *Lactose hydrolysis*, w*hey and lactose processing*, in Zadow, J.G. editor, London, New York: Elsevier, 361-408.
7. Jelen, P.J. (1993). Lactose hydrolysis using sonicated dairy cultures. *Bulletin of the International Dairy Federation,* 289, 54-56.
8. Kim, I.H.; and Chang, H.N. (1983). Variable-volume hollow-fibre enzyme reactor with pulsatile flow. *AIChE Journal,* 29(6), 910-914.
9. Walsh, M.K.; and Swaisgood, H.E. (1993). Characterization of a chemically conjugated β-galactosidase bioreactor. *Journal of Food Biochemistry,* 17(4), 283-292.
10. Heng, M.H.; and Glatz, C.E. (1994). Ion exchange immobilization of charged β-galactosidase fusions for lactose hydrolysis. *Biotechnology and Bioengineering,* 44(6), 745-752.
11. Fujikawa, H.; and Itoh, T. (1997). Differences in the thermal inactivation kinetics of *Escherichia coli* β-galactosidase in vitro and in vivo. *Biocontrol and Science,* 2(2), 73-78.

12. Sungur, S.; and Yildirim, O. (1999). Batch and continuous hydrolysis of lactose using β-galactosidase immobilised on gelatine-CMC. *Polymer Plastic Technology and Engineering,* 38(4), 821-829.
13. Harju. M. (1987). Lactose hydrolysis, *Bulletin of the International Dairy Federation,* 212, 50-54.
14. Lilly, M.; and Dunnill, P. (1976). Immobilized-enzymes reactors. *Methods of Enzymology,* Immobilized Enzyme*,* 44, 717-738.
15. Papathanassiou, T.D.; Kalogerakis, N.; and Behie, L.A. (1988). Dynamic modelling of mass transfer phenomena with chemical reaction in immobilised-enzyme bioreactors. *Chemical Engineering Science*, 43(7), 1489-1498.
16. Lortie, R.; and Thomas, D. (1986). Heterogeneous one-dimensional model for fixed bed enzyme reactors. *Biotechnology and Bioengineering,* 28(8), 1256-1260.
17. Weetall, H.; Havewala, N.B.; Pitcher Jr., W.H.; Detar, C.C.; Vann, W.P.; and Yaverbaum, S. (1974). The preparation of immobilized lactase and its use in enzymatic hydrolysis of acid whey. *Biotechnology and Bioengineering,* 16(3), 295-313.
18. Friend, B.A.; and Shahani, K.M. (1982). Characterization and evaluation of *Aspergillus oryzae* lactase coupled to regenerable support. *Biotechnology and Bioengineering,* 24(2), 329-345.
19. Olafadehan, O.A.; Aribike, D.S.; and Adeyemo, A.M. (2009). Mathematical modeling and simulation of steady state plug flow for lactose-lactase hydrolysis in fixed bed. *Theoretical Foundations of Chemical Engineering*, 43(1), 58-69.
20. Olafadehan, O.A. (1989). *The transient characteristics of a packed bed tubular reactor for lactose-lactase hydrolysis*, B.Sc. Thesis, Lagos, University of Lagos, Nigeria.
21. Wehner, J.F.; and Wilhelm, R.H. (1956). Boundary conditions of flow reactor. *Chemical Engineering and Science,* 6(2), 89-93.
22. Olafadehan, O.A. (2000). *Modelling of multicomponent adsorption and reaction in porous media*. Ph. D. Dissertation, Lagos: University of Lagos, Nigeria.
23. Hinberg, I.; Korus, R.; and O'Driscoll, K.F. (1974). Gel entrapped enzymes: kinetic studies of immobilized β-galactosidase. *Biotechnology and Bioengineering,* 16(7), 943-963.
24. Mahoney, R.R.; and Whitaker, J.R. (1978). Stability and enzymatic properties of β-galactosidase from *Kluyveromices fragilis. Journal of Food Biochemistry,* 1(4), 327-350.
25. Engasser, J.M.; and Horvath, C. (1976). Diffusion and kinetics with immobilized enzymes. *Applied Biochemical and Bioengineering,* 1, 128-328.
26. Olafadehan, O.A.; and Susu, A.A. (2004). Modeling and simulation of liquid-phase ternary adsorption in activated carbon column. *Industrial and Engineering Chemistry Research,* 43(25), 8107-8116.
27. Geankoplis, C.J. (2002). *Transport processes and unit operations*. 3rd Ed. Prentice-Hall of India, New Delhi-110001.

28. Carrara, C.R.; and Rubiolo, A.C. (1997). A method for evaluating lactose hydrolysis in a fixed-bed reactor with β-galactosidase immobilized on chitosan. *Chemical Engineering Journal,* 65(2), 93-98.
29. Carrara, C.R.; and Rubiolo, A.C. (1994). The immobilization of β-galactosidase on chitosan. *Biotechnology Progress,* 10(2), 220-224.
30. Carrara, C.R.; and Rubiolo, A.C. (1996). Determination of kinetics parameters for free and immobilized β-galactosidase. *Process Biochemistry,* 31(3), 243-248.
31. Hassan, M.M.; and Beg, S.A. (1987). Theoretical analysis of a packed-bed biological reactor for various reaction kinetics. *The Chemical Engineering Journal,* 36(2), B15-B27.